Unraveling the Na,K-ATPase α_4 Subunit Assembling Induced by Large Amounts of $C_{12}E_8$ by Means of Small-Angle X-ray Scattering

Leandro Ramos Souza Barbosa,*,† Carolina Fortes Rigos,‡ Juliana Sakamoto Yoneda,‡ Rosangela Itri,† and Pietro Ciancaglini‡

Instituto de Física da Universidade de São Paulo, Cx. Postal 66318, CEP 05315-970 - São Paulo, SP, Brazil, and Departamento Química, FFCLRP-USP - 14040-901, Ribeirão Preto, SP, Brazil

Received: February 13, 2010; Revised Manuscript Received: June 16, 2010

In the current work, we studied the effect of the nonionic detergent dodecyloctaethyleneglycol, $C_{12}E_8$, on the structure and oligomeric form of the Na,K-ATPase membrane enzyme (sodium−potassium pump) in aqueous suspension, by means of small-angle X-ray scattering (SAXS). Samples composed of 2 mg/mL of Na,K-ATPase, extracted from rabbit kidney medulla, in the presence of a small amount of $C_{12}E_8$ (0.005 mg/mL) and in larger concentrations ranging from 2.7 to 27 mg/mL did not present catalytic activity. Under this condition, an oligomerization of the α subunits is expected. SAXS data were analyzed by means of a global fitting procedure supposing that the scattering is due to two independent contributions: one coming from the enzyme and the other one from $C_{12}E_8$ micelles. In the small detergent content (0.005 mg/mL), the SAXS results evidenced that Na,K-ATPase is associated into aggregates larger than $(\alpha\beta)_2$ form. When 2.7 mg/mL of $C_{12}E_8$ is added, the data analysis revealed the presence of α_4 aggregates in the solution and some free micelles. Increasing the detergent amount up to 27 mg/mL does not disturb the α_4 aggregate: just more micelles of the same size and shape are proportionally formed in solution. We believe that our results shed light on a better understanding of how nonionic detergents induce subunit dissociation and reassembling to minimize the exposure of hydrophobic residues to the aqueous solvent.

1. Introduction

Nonionic detergents and specifically fatty alcohol ethoxylates have been largely used for the extraction and purification of membrane proteins due to their selectivity and efficiency.[1] However, approaches that attempt to rationalize the relationship between the protein/detergent molar ratio and the physicochemical properties of the system are scarce.[2−4] Thus, understanding the detergent effects on the structural properties of specific membrane proteins is highly relevant for the evaluation and interpretation of several experimental results.

In the past few years, some of us have been working with the enzyme Na,K-ATPase extracted from the outer medulla of rabbit kidney, by using the nonionic detergent dodecyloctaethyleneglycol, $C_{12}E_8$,[5−7] although the enzyme can also be purified from several other protein-rich tissues.[8−12] Na,K-ATPase is a P-type family member of active transport proteins that is present in the plasma membrane of all animal cells. During the multistep reaction sequence, the enzyme complex undergoes a conformational change between two main reactive states, E_1 and E_2, in which 3 Na^+ ions and 2 K^+ ions are transported through the plasma membrane, respectively. This establishes a transmembrane potential difference.[13−15] The enzyme has an additional signal transduction function that results in cell growth and adhesion modulation,[16] as well as in the programmed cell death process (apoptosis).[17,18] However, the precise role of the proteins in the cell death still needs to be elucidated. Further, the signaling by the Na,K-ATPase is regulated by the steroid hormone ouabain. Nevertheless, the mechanisms by which the activity of the enzyme is regulated remain obscure.[16,19]

It is well established that the enzyme complex consists of two polypeptide chains, known as the α-subunit or catalytic chain (~110 kDa) and the β-subunit (35−50 kDa). The former is responsible for the enzymatic activity of the complex,[6,20] whereas the latter may also play a role in the catalytic reaction and ion-pumping mechanism,[20,21] besides its structural function. A third γ-subunit is a small hydrophobic protein (7−12 kDa) that is associated with the Na,K-ATPase in the kidney. Although not essential for either catalytic activity or for ion transport, the γ-subunit acts as a kinetic regulator.[22,23] It has been demonstrated that the $\alpha\beta$ unit of the Na,K-ATPase is capable of both ATP hydrolysis and active ion transport,[24−27] although there is some evidence that suggests that the enzyme normally self-associates as $(\alpha\beta)_2$ dimers[13,15,28−30] or as $(\alpha\beta)_4$ tetramers.[31−34] These data are supported by kinetic measurements with different nucleotide analogues that have revealed interactions between as many as four nonidentical binding sites.[15,16,34]

Previously, some of us have demonstrated that Na,K-ATPase, at small concentrations (<0.5 mg/mL) and in the presence of 0.005 mg/mL of $C_{12}E_8$, is found majorly in the $(\alpha\beta)_2$ form.[35] However, the Na,K-ATPase activity of all mentioned forms is lost for $C_{12}E_8$ concentrations above the critical micellar concentration, CMC, of 0.053 mg/mL.[36] Such a fact was attributed to the α and β subunits dissociation.[35,37,38] Moreover, once dissociated, an $\alpha-\alpha$ oligomerization must take place,[34,39,40] with no detectable activity for the α_n aggregate.

To check the detailed influence of the $C_{12}E_8$ on the Na,K-ATPase form, as well as the assumption of α_n self-aggregation, the current work is carried out, by means of small-angle X-ray scattering (SAXS). Such a technique is a powerful tool to study protein conformations in solution.[41] In this way, solutions of 2

* Corresponding author. E-mail: lbarbosa@if.usp.br. Phone: 55 11 30916814. Fax: 55 11 30916749.
† Instituto de Física da Universidade de São Paulo.
‡ Departamento Química, FFCLRP-USP.

10.1021/jp1013829
Published on Web 08/17/2010

mg/mL of Na,K-ATPase under the influence of increasing $C_{12}E_8$ concentrations are investigated as described below.

2. Materials and Methods

2.1. Materials. All solutions were prepared using pure apyrogenic water (Millipore Direct-Q), and all reagents were of the highest commercial purity available. TCA, Tris, HEPES, ATP, BSA, and $C_{12}E_8$ were from Sigma. EDTA, potassium chloride, sodium chloride, and magnesium chloride were all of research grade from Merck.

2.2. Preparation of Rabbit Kidney Medulla Na,K-ATPase. Solubilized Na,K-ATPase, $(\alpha\beta)_2$ form with relative molecular mass of 320 kDa, was isolated and purified from the dark red outer medulla of the kidney of adult New Zealand white rabbits as previously described by Santos et al.[5]

2.3. ATPase Activity Measurement. ATPase activity was assayed discontinuously at 37 °C in a final volume of 1.0 mL by quantification of phosphate release as described by Heinonen and Lahti.[42] The reaction was initiated by addition of the enzyme and was stopped with 0.5 mL of cold 30% TCA. Samples were centrifuged at 4000*g* prior to phosphate determination. Standard assay conditions were 50 mM HEPES buffer, pH 7.5, containing 3 mM ATP, 10 mM KCl, 5 mM $MgCl_2$, and 50 mM NaCl. The protein concentration was maintained constant at 0.1 mg/mL, and the detergent concentration was varied between 0.005 and 1.00 mg/mL. Assays were performed in triplicate using three separate enzyme preparations. Controls without added enzyme were included in each experiment to quantify nonenzymatic hydrolysis of the substrate. The initial rates of hydrolysis were constant for at least 30 min, provided that less than 5% of substrate was consumed in the reaction.[6]

2.4. SAXS Measurements and Data Analysis. ***2.4.1. SAXS Experiments.*** The experiments were performed at the National Synchrotron Light Laboratory (LNLS, Campinas, Brazil) at room temperature of 298 K, with radiation wavelength $\lambda = 1.488$ Å and sample-to-detector distance of 1360 mm. Samples were set between two mica windows and a 1 mm spacer, handled in a liquid sample-holder. This was placed perpendicular to the primary X-ray beam. The obtained curves (data collection of 10 min) were corrected for detector homogeneity (bidimensional position-sensitive detector) and normalized by taking into account the decrease of the X-ray beam intensity during the experiment. The parasitic background from the buffer solution was subtracted, considering the sample's attenuation.

Solutions of 2 mg/mL of Na,K-ATPase were prepared in 50 mM HEPES buffer at pH 7.4, and added $C_{12}E_8$ concentrations of 2.7, 5.4, 8.1, 13.5, 18.9, and 27.0 mg/mL that correspond to the detergent/enzyme molar ratio of 800, 1600, 2400, 4000, 5600, and 8000, respectively. It is important to mention that there is always a small residual amount of $C_{12}E_8$ that remains in the solution after the extraction and purification of the enzyme. Such a residual concentration amounts to 0.005 mg/mL,[5,35] i.e., below the CMC value.[36]

2.4.2. SAXS theory. The SAXS intensity, $I(q)$, of an isotropic solution of noninteracting scattering particles can be described as[43−45]

$$I(q) = kn_pP(q) \quad (1)$$

where n_p corresponds to the particle number density and k is a normalization factor related to the instrumental effects ($q = 4\pi \sin \theta/\lambda$ is the scattering vector, 2θ being the scattering angle). $P(q)$, eq 1, is the orientational average of the particle form factor and gives information on the scattering particle size and shape.

A Fourier transform connects $P(q)$, and hence $I(q)$, to the pair distance distribution function, $p(r)$.[43−45] In this way, such a function is model-free and represents the probability of finding a pair of small elements at a distance r within the entire volume of the scattering particle, providing information about the scattering particle shape and its radius of gyration, R_g.[45] Moreover, the particle maximum dimension, D_{max}, is accounted for a certain r value where $p(r)$ goes to zero. In the current work, we made use of the GNOM software[46] to generate the $p(r)$ functions from the experimental $I(q)$ curves.

Concerning the model-dependent SAXS data analysis, the micelle-like aggregates are modeled as prolate ellipsoids,[47] the shortest semiaxis being on the order of paraffinic chain length, R_{par}, whereas the largest semiaxis is νR_{par}, with ν equal to the micellar axial ratio. The model assumes that the micelle is constituted by two shells of different electron densities: an inner core of paraffinic moiety, with electron density $\rho_{par} = 0.275$ e/Å^3, and an external shell, surrounding the core, with a respective polar headgroup thickness σ that includes the hydration water, and with electron density ρ_{pol}, relative to the continuous medium (buffer solution with electron density similar to that of water $\rho_w = 0.334$ e/Å^3). Details are described elsewhere.[48,49]

Concerning the SAXS curves from the solutions that contained the solubilized Na,K-ATPase, in the presence of added $C_{12}E_8$ (above CMC), they are modeled as a sum of two different contributions: one coming from the enzyme and the other one from $C_{12}E_8$ micelles. Hereafter, we tried to use different model geometries for the enzyme, such as cylinder, prolate, and oblate ellipsoids. The best theoretical fitting to the data was achieved when the scattering of an effective oblate ellipsoid was employed to simulate the enzyme scattering. In this case, the fitting parameters were R_{prot} (major semiaxes), the anisometry ν_{prot} (the protein axial ratio), and the enzyme electron density, ρ_{prot}. The overall data set was thus analyzed by making use of the Global fitting procedure.[50−52] Such a methodology performs a χ^2 minimization with a simulating annealing process,[53] changing the free parameters until χ^2 reaches a minimum value. It allows the linkage among different fitting parameters from distinct scattering curves. This process can improve the uniqueness of the final solution.

To better explore our results, we also tried to use the known crystallographic structure of the α subunit[54] (entry 3KDP from the pdb Web site) to propose a possible self-assembling structure of the α_n aggregate. To check this possibility, Monte Carlo Simulations (MCS)[55] were used to calculate the scattering curve of such a proposed structure.

3. Results and Discussion

Detergents are ubiquitous and necessary reagents for the study of membrane protein biochemistry. They are commonly used as mimics of lipid bilayers due to their self-assembling properties. Moreover, a detergent-solubilized system is usually required to keep the transmembrane portion of a membrane protein away from water, avoiding protein aggregation. Nevertheless, it is important to mention that it is difficult to keep a solubilized membrane protein on its native conformational state.[35,38,56]

Figure 1 shows the SAXS curves of 2 mg/mL of Na,K-ATPase solution at pH 7.4 in the presence of increasing $C_{12}E_8$ concentration: 0.005, 2.7, 5.4, 8.1, 13.5, 18.9, and 27.0 mg/mL of $C_{12}E_8$ (Figure 1A), as well as a typical SAXS curve of 10 mg/mL of $C_{12}E_8$ micelle-like aggregates (Figure 1B) for comparison.

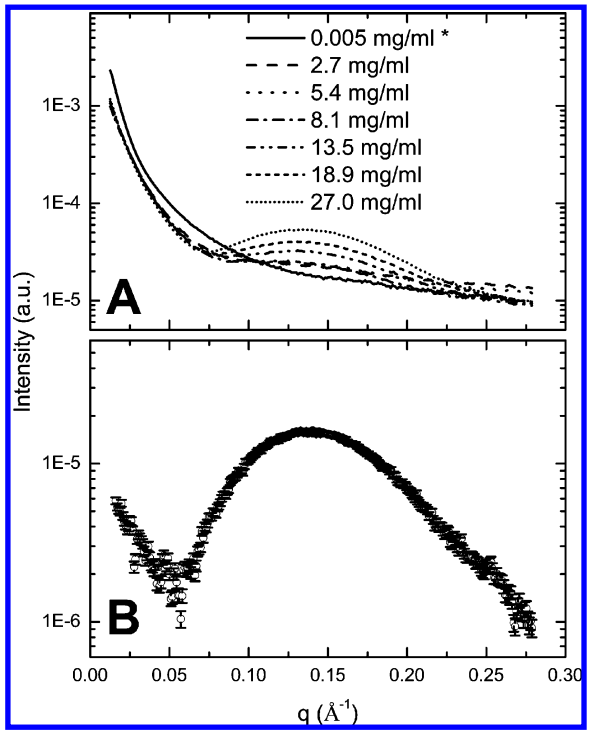

Figure 1. SAXS curves from: (A) 2 mg/mL of Na,K-ATPase in the absence and presence of increasing $C_{12}E_8$ concentration and (B) 10 mg/mL of $C_{12}E_8$. * Such a detergent concentration corresponds to a small residual amount of $C_{12}E_8$ that remains in solution after the extraction and purification of the enzyme.[5,35]

As one can see, the scattering curve of the enzyme suspension containing only the residual $C_{12}E_8$ concentration has a monotonic decay, whereas a broad peak around 0.13 $Å^{-1}$ takes place over the SAXS curve in detergent concentrations above CMC. Such a broad peak can be attributed to the scattering of the $C_{12}E_8$ micelles in solution as shown in Figure 1B.[48,49,57]

It is not trivial to crystallize membrane proteins, generally due to their hydrophobic region. In the case of Na,K-ATPase, there is a further challenge once it is a multidomain enzyme. In fact, Na,K-ATPase in solution can be in equilibrium with its self-associated forms such as $(\alpha\beta)$, $(\alpha\beta)_2$, .., $(\alpha\beta)_n$.[35] Despite these obstacles, the α subunit of Na,K-ATPase (from pig renal) was successfully crystallized by Pedersen et al.[54] Recently, Shinoda at al.[58] obtained the crystal structure of Na,K-ATPase, including part of the β subunit from the $(\alpha\beta)$ oligomer. Nevertheless, the crystallographic structure of the whole active form of Na,K-ATPase still needs to be solved.

So, to interpret our SAXS curves, we started the data analysis by using the available crystallographic structure of Na,K-ATPase to generate a theoretical SAXS curve (data not shown). Unfortunately, the theoretical curve was not able to reproduce our SAXS data. The mismatch occurs in the beginning of the scattering curve, indicating that larger aggregates are present in solution.[59]

To proceed with the data analysis, we thus focused our attention on the scattering curve of 2 mg/mL enzyme in the presence of 0.005 mg/mL of $C_{12}E_8$ through the $p(r)$ function that is a model-free analysis. Figure 2A displays the best fitting to the experimental data obtained through IFT methodology by using the GNOM software,[46] while the corresponding $p(r)$ function is shown in the inset. According to the $p(r)$ function, the purified enzyme has, at least, a maximum dimension, D_{max}, of 400 ± 16 Å, with radius of gyration of 127 ± 5 Å, and is slightly anisometric, once the maximum frequency of distances in the $p(r)$ function is around 150 ± 5 Å.

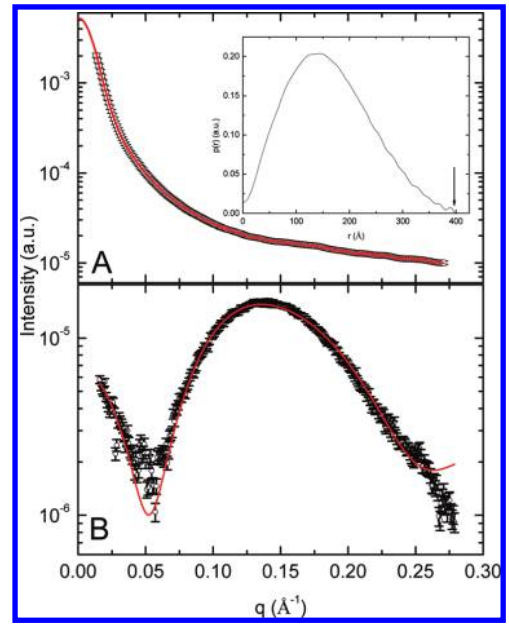

Figure 2. (A) SAXS curve of 2 mg/mL of Na,K-ATPase in the presence of 0.005 mg/mL of $C_{12}E_8$ along with the best fit obtained with the Indirect Fourier Transformation (IFT) methodology through GNOM software.[46] The pair distance distribution function can be appreciated in the inset. (B) SAXS curve of 10 mg/mL of $C_{12}E_8$ micelles along with the best fit obtained with the prolate ellipsoidal model. See text for details.

TABLE 1: Values of the Ellipsoid Fitting Parameters Obtained from the Scattering Curves of Samples Composed of $C_{12}E_8$ Ranging from 2.7 to 27 mg/mL, in the Absence and Presence of 2 mg/mL of Na,K-ATPase[a]

	$C_{12}E_8$ 10 mg/mL	micelle + enzyme	enzyme
R_{par} (Å)	17.2 ± 1.2	17.8 ± 1.1	110 ± 10[b]
σ_{pol} (Å)	9.1 ± 1.0	8.6 ± 1.1	–
ρ_{pol} (e/Å^3)	0.37 ± 0.01	0.37 ± 0.01	0.40 ± 0.01
ν	2.0 ± 0.2	2.0 ± 0.2	0.30 ± 0.05

[a] Legend: R_{par} = shortest paraffinic axis, σ_{pol} = polar shell thickness, ρ_{pol} = polar shell electron density, ν = axial ratio between the largest and the shortest paraffinic axis. [b] It is important to mention that the protein aggregate was modeled as a homogeneous effective oblate ellipsoid, thus R_{par} corresponds, indeed, to the effective oblate ellipsoid semi-axis, R.

Concerning the $C_{12}E_8$ micelle-like aggregates, Figure 2B shows the SAXS data of 10 mg/mL of $C_{12}E_8$, at pH 7.4, along with the best model fitting assuming that the scattering of the micelle resembles that of a prolate ellipsoid, as described in the Materials and Methods section. As one can see in the figure, such a model fits quite well the experimental data with fitting parameters: hydrophobic radius of 17.2 ± 1.2 Å, polar shell thickness and electronic density equal to 9.1 ± 1.0 Å and 0.37 ± 0.01 e/Å^3, respectively, axial ratio of 2.0 ± 0.2, and aggregation number of 120 ± 25, in good agreement with previous results.[57] All results are displayed in Table 1.

On the other hand, Figure 3 shows the $p(r)$ functions of the systems composed by Na,K-ATPase in the presence of $C_{12}E_8$ concentrations above CMC. The oscillation evidenced in the r < 80 Å region in the $p(r)$ function (arrow on Figure 3) is due to the presence of micelles in solution.[60] Moreover, the oscillation amplitude increases with $C_{12}E_8$ concentration. In a general way, the $p(r)$ functions are quite similar among them, suggesting that the overall shape of the protein complex must be similar. In all cases, the maximum dimension of the protein is reduced from 400 ± 15 Å to 300 ± 12 Å in the presence of $C_{12}E_8$

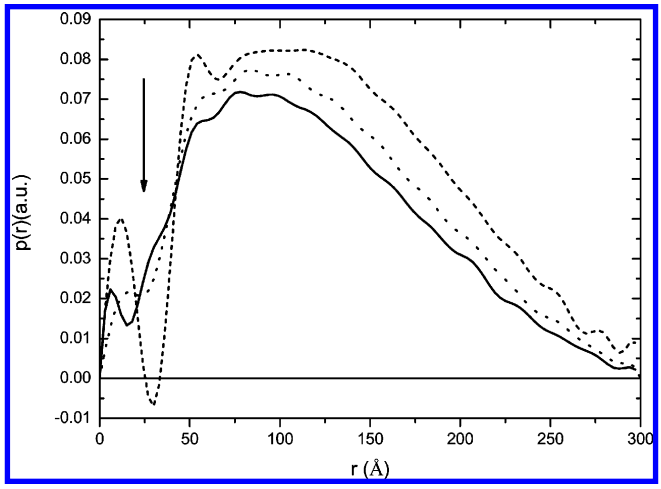

Figure 3. $p(r)$ functions of the systems composed by 2 mg/mL of Na,K-ATPase in the presence of 2.7 (solid line), 8.3 (dotted line), and 27.0 mg/mL (dashed line). The arrow indicates the influence of $C_{12}E_8$ micelles in the $p(r)$ function.

concentrations above the CMC. Concomitantly, the maximum of frequencies of distances in the $p(r)$ function also reduces to *circa* 100 ± 8 Å.

Thus, it is possible to infer that the protein scattering and, as a consequence, its maximum dimension are independent of the $C_{12}E_8$ concentration from 2.7 to 27 mg/mL. Changes in the scattering curves are mainly due to the scattering of micelles. To better understand these results, we now analyze these set of experimental curves, i.e., Na,K-ATPase, in the presence of increasing $C_{12}E_8$ concentration using GENFIT software,[50,52,55] as follows. To do so, we assumed that the scattering curves are due to two different contributions: one coming from the protein represented as an effective oblate ellipsoid (see Materials and Methods for details) and the other one from the micelles present in solution, modeled as prolate ellipsoids. The main difference among these SAXS curves lies on the $C_{12}E_8$ concentration and, as a consequence, on the number of free micelles in solution.

So, Figure 4 presents the SAXS curves of Na,K-ATPase in the presence of increasing $C_{12}E_8$ concentration along with the best fittings. The micellar structural parameters are similar to those found for the enzyme-free $C_{12}E_8$ micelles in solution (Figure 2B) with R_{par} and ν equal to 17.8 ± 1.1 Å and 2.0 ± 0.2, respectively. The polar shell thickness and the corresponding electron density are equal to 8.6 ± 1.1 Å and 0.37 ± 0.01 e/Å^3, respectively. All results are included in Table 1. Therefore, the $C_{12}E_8$ micelle features are similar, regardless of the presence of the purified enzyme in the solution.

Regarding the protein structural parameters, the fitting results indicate that it can be modeled as an oblate ellipsoid with longest semiaxis of 110 ± 10 Å, in agreement with the maximum frequency of distances of the $p(r)$ function, and axial ratio equal to 0.30 ± 0.05 (inset on Figure 4) and $\rho_{prot} = 0.40 \pm 0.01$ e/Å^3 for all scattering curves. The latter value is compatible with the mean electron density of several proteins.[50,52,55]

Noteworthily, the global fitting analysis evidences an increase in the number of $C_{12}E_8$ micelles in solution, at the same ratio as the increasing surfactant concentration. Therefore, our results indicate that the presence of 2.7 mg/mL of $C_{12}E_8$ is enough to promote a reduction of the enzyme aggregate dimensions. Furthermore, increasing the surfactant concentration, the enzyme aggregate remains unaltered, whereas more micelles are formed in the solution.

In terms of what kind of enzyme aggregate could be formed, it is well-known that when Na,K-ATPase is dissociated the α−α

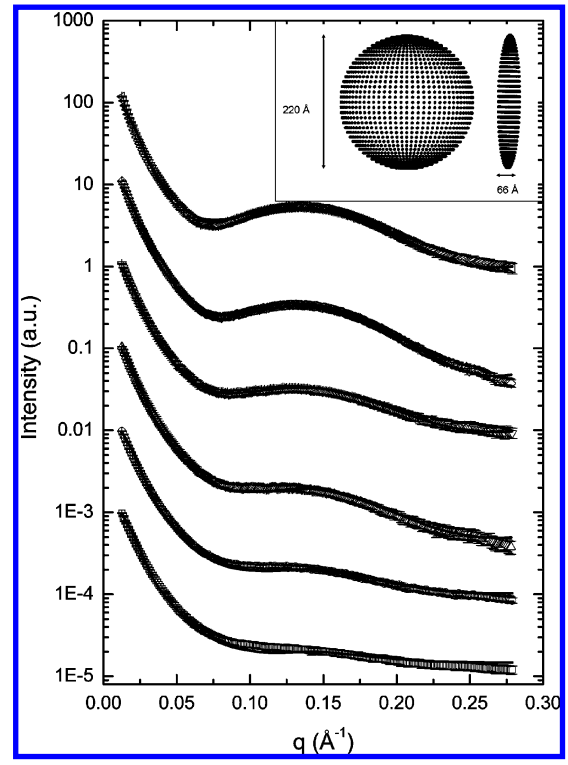

Figure 4. SAXS curves of Na,K-ATPase in the presence of 2.7, 5.4, 8.1, 13.5, 18.9, and 27.0 mg/mL of $C_{12}E_8$, along with the best fitting obtained with the sum of the oblate (representing the solubilized protein aggregate) and a prolate (representing the micelles in solution) ellipsoidal models. The SAXS curves are shifted for clarity. The oblate ellipsoid used to fit these SAXS curves, along with its dimension, can be appreciated in the inset.

oligomerization (α_n) may take place.[34,39,40] It is important to mention that α_n has no detectable activity. This is exactly our case, once no Na,K-ATPase activity was observed for samples composed of 2 mg/mL of enzyme and $C_{12}E_8$ concentration varying from 2.7 to 27.0 mg/mL. To check the α_n aggregation possibility, we calculated the scattering curve of the α-dimer and α-tetramer forms. As mentioned earlier in the text, the partial crystallographic structure of Na,K-ATPase was recently determined by Pedersen et al.[54] We used such a structure (entry 3KDP from pdb Web site) to initially calculate the corresponding theoretical SAXS intensity of the α_2 form, by means of GENFIT software.[50−52] Such an aggregate does not fit well the experimental SAXS curve (data not shown).

On the other hand, Figure 5 shows the SAXS curve of 2 mg/mL of Na,K-ATPase in the presence of 27 mg/mL, along with the corresponding scattering curve of an α_4 aggregate depicted in Figure 6, the scattering curve of $C_{12}E_8$ free micelles, as well as the sum of these two contributions. Figure 6 shows the schematic representation of the oblate ellipsoid obtained with the SAXS data fitting (Figure 4) with the proposed α_4 aggregate. It is worth mentioning that, even though we have tried different relative positions for the tetrameric form, only the α_4 aggregation model proposed here fits well the scattering curve.

Therefore, this methodology was able to reproduce very well the SAXS curves, indicating that the protein is probably in the α_4 state. It is important to mention that in this methodology the β subunit is not considered in the SAXS data analysis. As far as we know, this subunit has one transmembrane α-helical moiety (with 27 residues), but it is mainly water-soluble (around 265 residues in the cytosolic region)[13] and has a smaller size (around 50 kDa[61]) as compared to α_4 (∼440 kDa). Moreover,

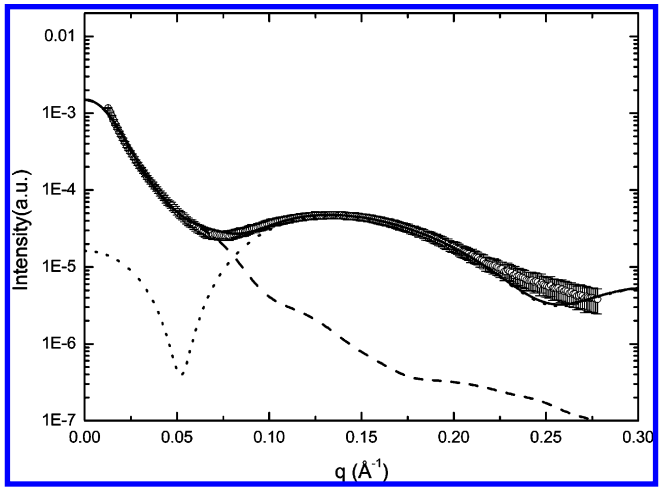

Figure 5. SAXS curve of 2 mg/mL of Na,K-ATPase in the presence of 27 mg/mL of $C_{12}E_8$ (open circles) along with the form factor of α_4 crystallographic structure (using the α subunit crystallized by Pedersen et al.[54] (dashed line), the $C_{12}E_8$ micelles (dotted line), and their sum (solid line)).

this domain is found at small concentrations (around 2 mg/mL). Due to these reasons, the SAXS signal of this structure was not detected in the SAXS curves under our experimental conditions. Thus, it is possible to neglect this contribution on the SAXS data analysis.

A similar thermoinactivation and aggregation process for Na,K-ATPase was also observed by Jorgensen and Andersen.[31] In that work, the authors suggested that inactivation/aggregation both in the soluble and in the membrane-bound state involves exposure of hydrophobic residues to solvent. In this way, associated with our previous data,[35,37,38] the instability of the soluble α may be related to inadequate length of the dodecyl alkyl chain of $C_{12}E_8$ for stabilization of protein hydrophobic domains that normally associate with alkyl chains of phospholipids in the membrane or associated with the β subunit. This instability results in irreversible α_4 aggregation that appears to be a consequence of protein denaturation.

4. Conclusions

In the present work, we studied how increasing $C_{12}E_8$/Na,K-ATPase molar ratios impacts the structural features of the enzyme. In fact, we observed that for $C_{12}E_8$ concentrations greater than 2.7 mg/mL, i.e., at 800 detergent molecules per enzyme, the latter loses, at least, 90% of its activity. It is well-known that the $(\alpha\beta)_n$ aggregate does not exist at this surfactant detergent level. Further, the influence of the detergent must lead to a dissociation of α and β subunits, followed by a self-assembling of the $\alpha-\alpha$ subunits.[35] Our SAXS results corroborate such a proposal, once the scattering of an α_4 aggregate fits quite well the experimental data. Moreover, as more detergent is added to the enzyme suspension, more micelles are formed, without disturbing the α_4 aggregate already existent. We believe that this information can improve our understanding about the action of the nonionic detergent on the extraction and purification of the Na,K-ATPase enzyme related to its functional structure.

Abbreviations. Trichloroacetic acid (TCA); tris[hydroxymethyl]aminomethane (Tris); *N*-(2-hydroxyethyl) piperazine-*N*′-ethanesulfonic acid (HEPES); adenosine 5′-triphosphate Tris salt (ATP); bovine serum albumin (BSA); dodecyloctaethyleneglycol ($C_{12}E_8$); ethylenediaminetetracetic acid (EDTA), critical micellar concentration (CMC).

Acknowledgment. The authors are in debt to Prof. Dr. Francesco Spinozzi and Prof. Dr. Paolo Mariani who provided GENFIT software. We also thank the National Laboratory of Synchrotron Light (LNLS, Campinas) for the SAXS measurements, as well as FAPESP, CAPES (Nanobitec-Brasil), and CNPq for the financial support given to our laboratories. LRSB and CFR received a FAPESP Pos-Doc fellowship, and JSY received CAPES Ms fellowship.

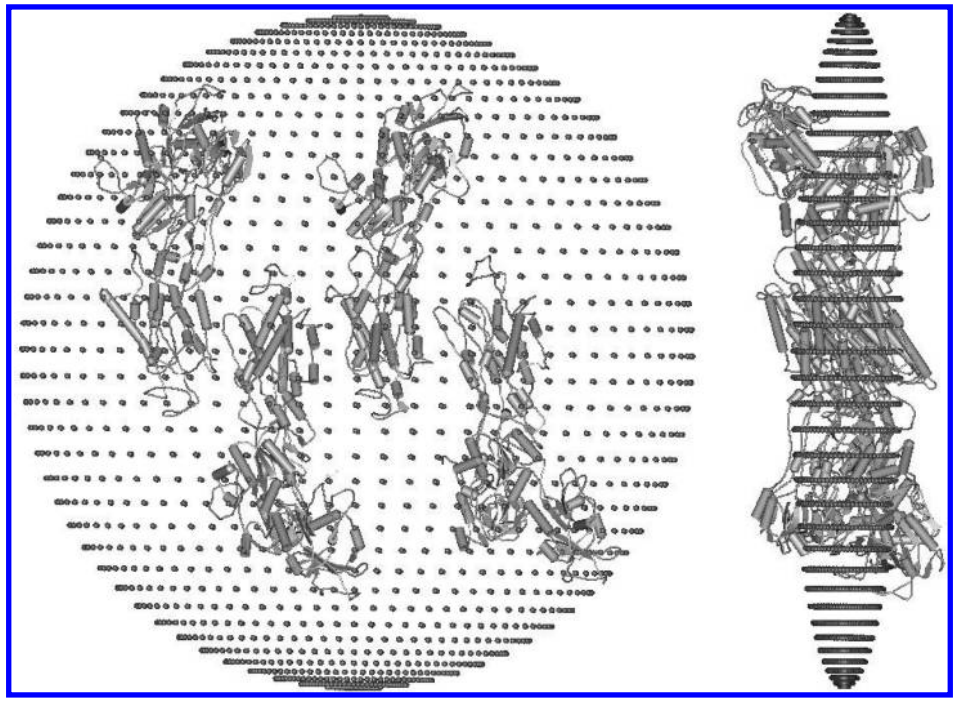

Figure 6. Schematic representation of the α_4 aggregate. The respective scattering curve can be appreciated in Figure 5 (dashed line). We also stress that the α_4 aggregate and the effective oblate ellipsoid displayed in Figure 4 have similar dimensions.

References and Notes

(1) Kalipatnapu, S.; Chattopadhyay, A. *IUBMB Life* **2005**, *57*, 505.
(2) Schurholz, T.; Gieselmann, A.; Neumann, E. *Biochim. Biophys. Acta* **1989**, *986*, 225.
(3) Berger, B. W.; García, R. Y.; Lenhoff, A. M.; Kaler, E. W.; Robinson, C. R. *Biophys. J.* **2005**, *89*, 452.
(4) Urbani, A.; Warne, T. *Anal. Biochem.* **2005**, *336*, 117.
(5) Santos, H. L.; Lamas, R. P.; Ciancaglini, P. *Braz. J. Med. Biol. Res.* **2002**, *35*, 277.
(6) Santos, H. L.; Ciancaglini, P. *Comp. Biochem. Physiol., Part B: Biochem. Mol. Biol.* **2003**, *135*, 539.
(7) Santos, H. L.; Rigos, C. F.; Ciancaglini, P. *Comp. Biochem. Physiol., Part C: Toxicol. Pharmacol.* **2006**, *142*, 309.
(8) Post, R. L; Kume, S.; Tobim, T.; Orcutt, B.; Sem, A. K. *J. Gen. Physiol.* **1969**, *54*, 306.
(9) Heimburg, T.; Esmann, M.; Marsh, D. *J. Biol. Chem.* **1997**, *272*, 25685.
(10) Lopina, O. D. *Biochemistry (Moscow)* **2001**, *66*, 1122.
(11) Rajasekaran, S. A.; Barwe, S. P.; Rajasekaran, A. K. *Semin. Nephrol.* **2005**, *25*, 328.
(12) Panayiotidis, M. I.; Bortner, C. D.; Cidlowski, J. A. *Acta Physiol. (Oxf).* **2006**, *187*, 205.
(13) Jorgensen, P. L.; Hakansson, K. O.; Karlish, S. J. D. *Annu. Rev. Physiol.* **2003**, *65*, 817.
(14) Horisberger, J. D. *Physiology (Bethesda)* **2004**, *19*, 377.
(15) Martin, D. W. *Semin. Nephrol.* **2005**, *25*, 282.
(16) Clarke, R. J. *Eur. Biophys. J.* **2009**, *39*, 3.
(17) Akiyama, M.; Ogura, M.; Iwai, M.; Iijima, M.; Numazawa, S.; Yoshida, T. *Hum. Cell.* **1999**, *12*, 205.
(18) Xiao, A. Y.; Wei, L.; Xia, S.; Rothman, S.; Yu, S. P. *J. Neurosci.* **2002**, *22*, 1350.
(19) Aperia, A. *J. Intern. Med.* **2007**, *261*, 44.
(20) Kaplan, J. H. *Annu. Rev. Biochem.* **2002**, *71*, 511.
(21) Hasler, U.; Wang, X. Y.; Crambert, G.; Beguin, P.; Jaisser, F.; Horisberger, J. D.; Geering, K. *J. Biol. Chem.* **1998**, *273*, 30826.
(22) Béguin, P.; Wang, X.; Firsov, D.; Puoti, A.; Claeys, D.; Horisberger, J. D.; Geering, K. *EMBO J.* **1997**, *16*, 4250.
(23) Garty, H.; Karlish, S. J. *Semin. Nephrol.* **2005**, *25*, 304.
(24) Ward, D. G.; Cavieres, J. D. *Proc. Natl. Acad. Sci. U.S.A.* **1993**, *96*, 5332.
(25) Ward, D. G.; Cavieres, J. D. *J. Biol. Chem.* **1996**, *271*, 12317.
(26) Martin, D. W.; Marecek, J.; Scarlata, S.; Sachs, J. R. *Proc. Natl. Acad. Sci. U.S.A.* **2000**, *97*, 3195.
(27) Takeda, K.; Kawamura, M. *Biochem. Biophys. Res. Commun.* **2001**, *280*, 1364.
(28) Thoenges, D.; Schoner, W. *J. Biol. Chem.* **1997**, *272*, 16315.
(29) Antolovic, R.; Hamer, E.; Serpersu, E. H.; Kost, H.; Linnertz, H.; Kovarik, Z.; Schoner, W. *Eur. J. Biochem.* **1999**, *261*, 181.
(30) Costa, C. J.; Gatto, C.; Kaplan, J. H. *J. Biol. Chem.* **2003**, *278*, 9176.
(31) Jorgensen, P. L.; Andersen, J. P. *Biochemistry* **1986**, *25*, 2889.
(32) Mahaney, J. E.; Girard, J. P.; Grisham, C. M. *FEBS Lett.* **1990**, *260*, 160.
(33) Taniguchi, K.; Kaya, S.; Abe, K.; Mardh, S. *J. Biochem.* **2001**, *129*, 335.
(34) Donnet, C.; Aristarkhova, E.; Sweadner, K. J. *J. Biol. Chem.* **2001**, *276*, 7357.
(35) Rigos, C. F.; Nobre, T. M; Zaniquelli, M. E. D.; Ward, R. J.; Ciancaglini, P. *J. Colloid Interface Sci.* **2008**, *325*, 478.
(36) Le Maire, M.; Champeil, P.; Moller, J. V. *Biochim. Biophys. Acta Biomembr.* **2000**, *1508*, 86.
(37) Rigos, C. F.; Santos, H. L.; Ward, R. J.; Ciancaglini, P. *Cell Biochem. Biophys.* **2006**, *44*, 438.
(38) Rigos, C. F.; Santos, H. L.; Yoneda, J. S.; Montich, G.; Maggio, B.; Ciancaglini, P. *Biophys. Chem.* **2010**, *146*, 36.
(39) Esmann, M. *Biochim. Biophys. Acta* **1984**, *787*, 81.
(40) Grinberg, A. V.; Gevondyan, N. M.; Grinberg, N. V.; Grinberg, V. Y. *Eur. J. Biochem.* **2001**, *268*, 5027.
(41) Koch, M. H. J.; Vachette, P.; Svergun, D. I. *Q. Rev. Biophys.* **2003**, *36*, 147.
(42) Heinonen, S. K.; Lathi, R. J. *Anal. Biochem.* **1981**, *113*, 313.
(43) Guinier, A.; Fournet, G. *Small Angle Scattering of X-Rays*; Wiley: New York, NY, 1955.
(44) Svergun, D. I.; Feigin, L. A. *Structure analysis by Small-angle X-ray and Neutron Scattering*; Plenum Press: New York, NY, 1987.
(45) Glatter, O.; Kratky, O. *Small Angle X-ray Scattering*; Academic Press: New York, NY, 1982.
(46) Semenyuk, A. V.; Svergun, D. I. *J. Appl. Crystallogr.* **1991**, *24*, 537.
(47) Marignan, J.; Basseraud, P.; Delord, P. J. *J. Phys. Chem.* **1986**, *90*, 645.
(48) Barbosa, L. R. S.; Caetano, W.; Itri, R.; Homem-De-Mello, P.; Santiago, P. S.; Tabak, M. *J. Phys. Chem B* **2006**, *110*, 13086.
(49) Caetano, W.; Barbosa, L. R. S.; Itri, R.; Tabak, M. *J. Colloid Interface Sci.* **2003**, *260*, 414.
(50) Sinibaldi, R.; Ortore, M. G.; Mariani, P. *J. Chem. Phys.* **2007**, *126*, 235101.
(51) Sinibaldi, R.; Ortore, M. G.; Mariani, P. *Eur. Biophys. J.* **2008**, *37*, 673.
(52) Barbosa, L. R. S.; Ortore, M. G.; Spinozzi, F.; Mariani, P.; Bernstorff, S.; Itri, R. *Biophys. J.* **2010**, *98* (1), 147.
(53) Press, W. H.; Teukolsky, S. A.; Flannery. B. P. *Numerical Recipes. The Art of Scientific Computing*; Cambridge University Press: Cambridge, U.K., 1994.
(54) Pedersen, B. P.; Buch-Pedersen, M. J.; Morth, J. P.; Palmgren, M. G.; Nissen, P. *Nature* **2007**, *450*, 1111.
(55) Ortore, M. G.; Spinozzi, F.; Mariani, P.; Panciaroni, A.; Barbosa, L. R. S.; Amenitsch, H.; Teinhart, K.; Olliver, J.; Russo, D. *J. R. Soc. Interface* **2009**, *6*, S619.
(56) Privé, G. G. *Methods* **2007**, *41*, 388.
(57) Rangel-Yagui, C. O.; Hsu, H. W. L.; Barbosa, L. R. S.; Caetano, W.; Pessoa Jr, A.; Tavares, L. C.; Itri, R. *Pharm. Dev. Technol.* **2007**, *12*, 183.
(58) Shinoda, T.; Ogawa1, H.; Cornelius, F.; Toyoshima1, C. *Nature* **2009**, *459*, 446.
(59) Vestergaard, B.; Groenning, M.; Roessle, M.; Kastrup, J. S.; van de Weert, M.; Flink, J. M.; Frokjaer, S.; Gajhede, M.; Svergun, D. I. *PloS Biol.* **2007**, *5*, 1089.
(60) Itri, R.; Amaral, L. Q. *J. Phys. Chem.* **1991**, *95*, 423.
(61) Skou, J. C.; Esmann, M. *J. Bioenerg. Biomembr.* **1992**, *24*, 249.

JP1013829